Current Handling Capability of the Neutral Point of a Three-Phase/Switch/Level Boost-Type PWM (VIENNA) Rectifier

JOHANN W. KOLAR, UWE DROFENIK, F.C. ZACH

Technical University Vienna, Power Electronics Section 359.5
Gusshausstraße 27, Vienna A-1040, Austria/Europe
Tel.: +43-1-58801-3833 Fax.: +43-1-505 88 70
e-mail: kolar@ps1.iaee.tuwien.ac.at

Abstract. In this paper the stationary operational behavior of a three-phase/switch/level PWM rectifier is analyzed for asymmetrical loading of the output partial voltages. For the considerations a sinusoidal mains current shape, resistive behavior of the mains current fundamental and constant pulse frequency are assumed. Based on analytical calculations it is shown that the average value of the neutral point current (which has to be formed for asymmetrical load) has an approximately linear dependency on the distribution of the overall relative on-time of the switching states of the system being redundant concerning the voltage formation between begin and end of a pulse half interval. The maximum admissible load of the neutral point (capacitive output voltage center point) is calculated. This load is given as a function of the amplitude of the mains current and the voltage transfer ratio of the system. The calculations are checked by results of a digital simulation of the system behavior. Furthermore, the increase of the rms value of the ripple of the mains current of the rectifier is analyzed as it results for forming of an average value of the neutral point current. As basis for comparison there is used the ripple rms value which results for harmonic-(sub)optimal control and negligible average value of the neutral point current. Finally, the current stress on the power semiconductors and on the output capacitors of the system are compiled in form of diagrams which can be applied directly for dimensioning the system.

1 Introduction

In [1] a three-phase/switch/level PWM rectifier system (cf. **Fig.1**) with low effects on the mains has been proposed. It has especially the following advantages as compared to conventional two-level converter systems:

- lower blocking voltage stress on the power semiconductors and
- lower rated power of the inductances connected in series on the mains side.

If the switching overvoltages are neglected, all valves of the rectifier system have to sustain only the stress of half the output voltage. Therefore, also for high output voltage (in the region of low and medium power) the application of power MOSFETs with low on-resistance and of diodes with low reverse recovery time is made possible. Furthermore, the three-level characteristic results in a better matching of the time shape of the voltages formed by the bridge legs to a given reference phase voltage time behavior. For given switching frequency and given harmonic rms value of the mains current we can, therefore, reduce the inductivity of the series inductances and/or increase the system power density as compared to two-level converters.

By inclusion of the capacitive center point of the output voltage into the system function two partial voltages of equal amount are available at the output of the rectifier system. For a further transformation or conversion of the total output voltage it is obvious, therefore, to consider the arrangement of two individual DC/DC converters which are supplied from a partial voltage each. As advantages we want to mention again a low blocking voltage stress on the valves and the generally higher power density for splitting up a converter into partial systems (e.g., connected in parallel at the output side and switched in opposite phase) [2]. Furthermore, for the requirement of low output voltages of the DC/DC converters the occurrence of extreme voltage transfer ratios is avoided due to the lower input voltage. (High voltage transfer ratios lead - for DC/DC converters with simple structures - in general to short on-times and, therefore, to a low utilization of the different power semiconductors; for isolation of the input and output circuits the coupling of the primary and secondary circuits is reduced due to the required higher turns ratio; this finally increases the system power loss.)

However, for realization of two partial systems under certain conditions the problem of a not ideal distribution of the total power to the partial voltages and/or a DC load on the output voltage center point can occur. With regard to a practical realization we have to raise the question, therefore, to what extent this center point current (impressed by the load side) can be compensated by proper control of the rectifier system and by which operating parameters the maximum allowable load on the voltage center point is determined. As side conditions we have to see there maintaining the symmetry of the partial voltages and a sinusoidal shape of the mains phase currents.

In this paper based on the analysis of the voltage space vectors and the center point currents resulting for the different switching states of the system shown in Fig.1 a control method is developed which gives a controllability of the DC component of the center point current (cf. **section 2**). The considerations are based on a sinusoidal mains current shape, resistive fundamental mains behavior of the system, symmetry of the output partial voltages and constant pulse frequency. It is shown that the local average value of the center point current (related to a pulse period) can be influenced by the distribution of the local overall on-time of the system switching states which are redundant concerning the voltage formation (cf. **section 3**). This partition has to be performed between begin and end of each pulse half period. The obtainable average value of the center point current is calculated analytically in dependency on the modulation depth and the mains current amplitude. The results of the analytical calculations are verified by a digital simulation of the system behavior. In **section 4** the influence of a change of the distribution of the local overall on-time of the redundant switching states on the rms value of the harmonics of the mains current is investigated. As the considerations show, the formation of a DC component of the center point current of the system is linked to an increase of the mains current harmonics. As basis for comparison we choose the harmonic rms value resulting for a symmetric distribution of the overall on-time of the redundant switching states between begin and end of a pulse half interval and/or zero average value of the center point current and/or suboptimal control of the system concerning the mains current harmonics. Finally, in **section 5** the increase of the stress on the power components for the formation of a DC component of the center point current and/or for asymmetric loading of the output partial voltages is analyzed. There is shown the current stress (average and rms values) on the power semiconductors and on the output capacitors in dependency on the mains current peak value, on the modulation depth and on the degree of load asymmetry in form of diagrams which directly can be used for dimensioning of the system.

2 Basic Considerations

Before we analyze the loading capability of the capacitively formed center point M of the output voltage U_O we want to briefly summarize the basics of the control of the system in the following (cf. sections 2.1 and 2.2). Furthermore, in section 2.3 the load-side center point current is calculated which results for asymmetric distribution of the output load to the output partial voltages. In section 2.4 the procedure for a digital simulation of the system is discussed.

2.1 Control of the Rectifier Input Voltage, Space Vector Modulation

With the assumption of a sinusoidal, symmetric mains voltage system according

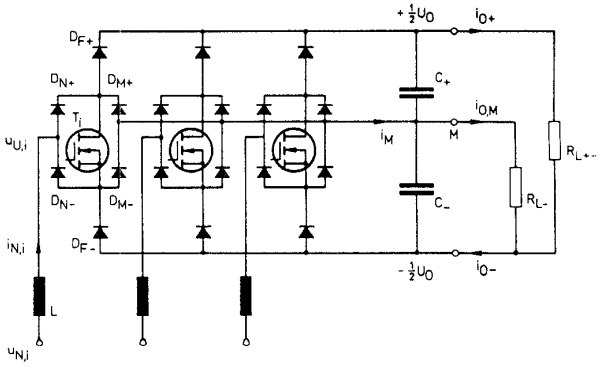

Fig.1: Basic structure of the power circuit of a three-phase/switch/level PWM (VIENNA) rectifier. R_{L-} denotes an asymmetric load of the partial output voltages of the system. In order to avoid a phase shift of the capacitive output voltage center point (neutral point) M one has to provide a DC component of the center point current $I_{M,\mathrm{avg}} = I_{O,M,\mathrm{avg}}$ by appropriate control of the rectifier system.

0-7803-3500-7/96/$ 5.00 © 1996 IEEE

to a space vector

$$\underline{u}_N = \hat{U}_N \exp j\varphi_N \qquad \varphi_N = \omega_N t \ , \tag{1}$$

(ω_N denotes the mains angular frequency) we have to provide a voltage space vector

$$\underline{u}_U^* = \hat{U}_U^* \exp j\varphi_U = \hat{U}_N \exp j\varphi_N - j\,\omega_N\,\underline{i}_N^* \tag{2}$$

in the average over a pulse period T_P at the input of the rectifier system in order to obtain an ideally sinusoidal shape of the mains current

$$\underline{i}_N^* = \hat{I}_N^* \exp j\varphi_N \tag{3}$$

being in phase with the mains voltage. The voltage space vectors $\underline{u}_U^* = \underline{u}_{U,(1)}$ and $\underline{i}_N^* = \underline{i}_{N,(1)}$ describe the fundamental contributions $u_{U,i,(1)}$ (with amplitude $\hat{U}_{U,(1)} = \hat{U}_U^*$) and/or $i_{N,i,(1)}$ (with amplitude $\hat{I}_{N,(1)} = \hat{I}_N^*$) of the phase quantities $u_{U,i}$, and/or $i_{N,i}$ ($i = R,S,T$). The space vectors being available for generating the vector $\underline{u}_U^*$ and their allocation to the switching states of the system (denoted by the triple of quantities (s_R, s_S, s_T) formed by the phase switching functions s_i) are determined according to

$$u_{U,i} = \begin{cases} \text{sign}\{i_{N,i}\}\frac{U_O}{2} & \text{if} \quad s_i = 0 \\ 0 & \text{if} \quad s_i = 1 \end{cases} \tag{4}$$

(cf. [3]) by the sign of the phase currents and/or by the angular position of current space vector $\underline{i}_N$. The conditions for $\varphi_N \in (-\frac{\pi}{6}, +\frac{\pi}{6})$ ($i_{N,R} > 0, i_{N,S} < 0, i_{N,T} < 0$) are shown in **Fig.2**. They are considered in the form of examples in the following. Basically we have at our disposal for the approximation of the continuous motion of $\underline{u}_U^*$ for each combination of signs of the three-phase currents only 8 out of a total of 19 different voltage space vectors of the system (cf. Fig.2 in [4]). The vector $\underline{u}_U^*$ therefore can be formed only in the average over a pulse period T_P. With regard to a best possible approximation one applies only those rectifier voltage space vectors $\underline{u}_{U,j}$ lying in the immediate vicinity of the vector tip or those switching states j which are assigned to the corner points of that triangular region of the space vector plane into which the tip of the vector $\underline{u}_U^*$ points (region marked by dots in Fig.2). Accordingly, there follows for the conditions of Fig.2 ($j = (000), (010), (011), (100)$)

$$\underline{u}_U^* = \delta_{(100)}\underline{u}_{U,(100)} + \delta_{(000)}\underline{u}_{U,(000)} + \delta_{(010)}\underline{u}_{U,(010)} + \delta_{(011)}\underline{u}_{U,(011)} \ . \tag{5}$$

The relative on-time δ_j of the switching states $j = (000)$ and (010) now can be calculated directly via an evaluation of simple geometrical relations (cf. Fig.4 in [5]). For the conditions shown in Fig.2 there follows

$$\begin{aligned} \delta_{(000)} &= \sqrt{3}M \sin(\frac{\pi}{3} - \varphi_U) - 1 \\ \delta_{(010)} &= \sqrt{3}M \sin\varphi_U \ . \end{aligned} \tag{6}$$

Furthermore we have

$$\delta_{(100)} + \delta_{(011)} = 1 - \delta_{(000)} - \delta_{(010)} = 2 - \sqrt{3}M \sin(\frac{\pi}{3} + \varphi_U) \ . \tag{7}$$

There, M denotes the modulation index of the pulse width modulation. M is defined by

$$M = \frac{\hat{U}_U^*}{\frac{1}{2}U_O} \ . \tag{8}$$

The limit to overmodulation is reached for

$$M_{\max} = \frac{2}{\sqrt{3}} \tag{9}$$

(equal as for 2-level converter systems). Within the scope of this paper only the system behavior for the region $M \in [\frac{2}{3}, \frac{2}{\sqrt{3}}]$ is investigated because this is especially interesting for a practical realization of the system.

In order to minimize the switching frequency of the system we now arrange the switching states within each pulse half period in such a way that the subsequent state can always be obtained by switching of only one bridge leg. If we select arbitrarily (100) as initial switching state there results within each pulse period T_P a switching sequence

$$\ldots|_{t_\mu=0}(100)\text{-}(000)\text{-}(010)\text{-}(011)|_{t_\mu=\frac{1}{2}T_P}(011)\text{-}(010)\text{-}(000)\text{-}(100)|_{t_\mu=T_P}\ldots \tag{10}$$

(if Fig.2 is used as basis); due to the requirement of a minimum number of switchings one has to reverse the sequence of the voltage space vectors $\underline{u}_{U,j}$ after each pulse half period.

For the further considerations it is important to point out that we always have a redundancy of 2 switching states of the system regarding the generation of $\underline{u}_U^*$. E.g., the switching states (100) and (011) lead to the same voltage space vector $\underline{u}_{U,(100)} = \underline{u}_{U,(011)}$ (if symmetrical output partial voltages of the system are assumed). By solving Eq.(5) with respect to the time weights δ_j we can, therefore, only calculate the sum $\delta_{(100)} + \delta_{(011)}$, but not a specific distribution of the overall on-time of the switching states (100) and (011) (cf. Eq.(7)). The distribution of the redundant voltage space vectors between begin and end of each pulse half period (cf. Eq.(10)) therefore constitutes a degree of freedom of the modulation method. This makes possible (as shown in the following) an influence on the average value of the current i_M being fed into the center point M.

Remark: A redundancy of switching states concerning the voltage generation is also given for *two*-level converters. There, a voltage space vector of length 0 results for both free-wheeling states (cf. e.g. Fig.5 in [6]).

We have to point out that the redundancy of the switching states regarding the voltage formation (equal position and equal absolute value of the formed voltage space vectors; e.g., $\underline{u}_{U,(100)} = \underline{u}_{U,(011)}$, cf. Fig.2) is given only for an exactly symmetric distribution of the output voltage $U_{C+} = U_{C-} = \frac{1}{2}U_O$ (cf. Fig.7 in [7]). This symmetry which is assumed for the further considerations is guaranteed by a control which influences the average value of i_M.

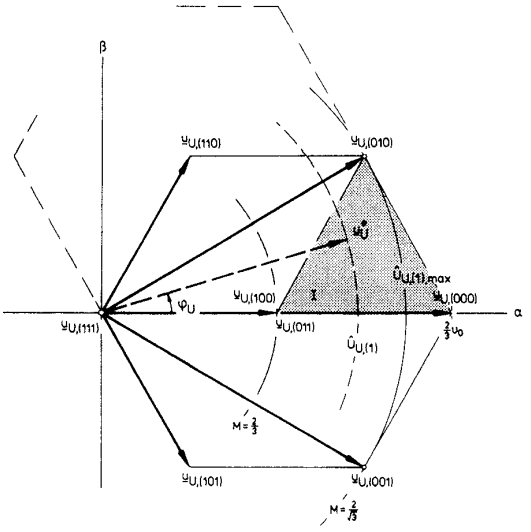

Fig.2: Voltage space vectors $\underline{u}_{U,j}$ which are associated to the switching states and/or the triple of the phase switching functions of the system $j = (s_R, s_S, s_T)$ for $\varphi_N \in (-\frac{\pi}{6}, +\frac{\pi}{6})$ and/or $i_{N,R} > 0$ and $i_{N,S}, i_{N,T} < 0$.

2.2 Controllability of the Center Point Current

For turning on of the power transistor of a phase ($s_i = 1$, $i = R,S,T$), a section of the relevant phase current $i_{N,i}$ is fed into the center point M. For the center point current resulting there for all phases we have therefore

$$i_M = s_R i_{N,R} + s_S i_{N,S} + s_T i_{N,T} \ . \tag{11}$$

The switching states j of the system, occurring within a pulse period (cf. Eq.(10)) therefore lead to the center point currents i_M as compiled in **Tab.1**.

s_R	s_S	s_T	i_M
1	0	0	$+i_{N,R}$
0	0	0	0
0	1	0	$+i_{N,S}$
0	1	1	$-i_{N,R}$

Tab.1: Center point current i_M in dependency on the converter switching state (s_R, s_S, s_T).

(cf. **Fig.3**). Because the center point of the system output voltage is formed only in a capacitive way there is of special interest now the local average value of the center point current being related to a pulse half period

$$i_{M,\text{avg}} = \frac{1}{\frac{1}{2}T_P} \int_0^{\frac{1}{2}T_P} i_M\{t_\mu\}\,\mathrm{d}t_\mu \tag{12}$$

(t_μ denotes a local time being counted within a pulse half period). $i_{M,\text{avg}}$ causes a shift of the center point potential (and, therefore, an increase of the blocking voltage stress of the power semiconductors). With Tab.1 there follows for the case considered here

$$i_{M,\text{avg}} = \delta_{(010)} i_{N,S} + (\delta_{(100)} - \delta_{(011)})\, i_{N,R} \ . \tag{13}$$

As becomes clear under consideration of the relation $i_{N,R}^* \geq |i_{N,S}^*|$ being valid in any case for $\varphi_N \in (-\frac{\pi}{6}, +\frac{\pi}{6})$, the distribution of the overall on-time $1-\delta_{(000)}-\delta_{(010)}$ (being given according to Eq.(7)) between the redundant switching states (100) and (011) (and/or between begin and end of a pulse half period) has essential influence on the local average value $i_{M,\text{avg}}$ of the center point current. In the following this distribution shall be denoted by the ratio

$$\rho_{--} = \frac{\delta_{--}}{\delta_{++} + \delta_{--}} \qquad \rho_{--} \in [0,1] \ . \tag{14}$$

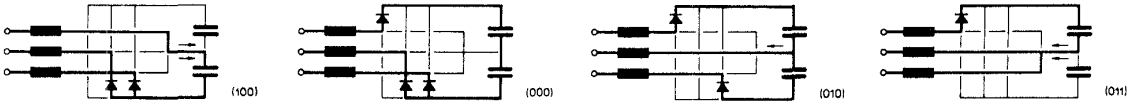

Fig.3: Conducting states of the rectifier system occurring within a pulse half period; the switching state of the system is denoted by the triple of the phase switching functions (s_R, s_S, s_T).

There, δ_{--} denotes the relative on-time of the respective redundant switching state (giving a negative center point current contribution) and δ_{++} denotes the relative on-time of the inverse redundant switching state (giving a positive center point current contribution). For the description given so far (as related to Fig.2) we have, therefore, the relationships $\delta_{++} = \delta_{(100)}$ and $\delta_{--} = \delta_{(011)}$. A symmetric distribution of the redundant switching states between begin and end of each pulse half period is given, therefore, for $\rho_{--} = 0.5$.

The controllabiltiy of $i_{M,\mathrm{avg}}$ by the parameter ρ_{--} is applied in general for the control of the symmetry of the output partial voltages, as described, e.g., in in [8] (cf. p. 496). If an unsymmetric distribution of the output voltage is given a transient average value $i_{M,\mathrm{avg}}$ of i_M is formed (via appropriate change of ρ_{--}) which corrects the asymmetry. If now (as shown in Fig.1), the load circuit has a connecting lead to the voltage center point M (and if there are the positive and negative partial voltage U_{C+} and U_{C-} loaded unevenly) we have to impress an average value $I_{M,\mathrm{avg}}$ of i_M also in the stationary case. This shall be treated in more detail in the following section.

2.3 Load on the Output Voltage Center Point for Unsymmetric Load Distribution

An unsymmetric distribution of the output power P_O of the system between positive and negative partial output voltages U_{C+} and U_{C-} can basically be represented by the simplified equivalent circuits of the load as shown in **Fig.4**(a) or

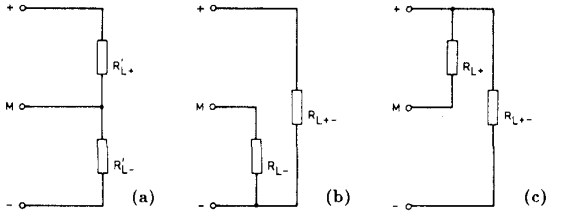

Fig.4: Basic equivalent circuits of the load circuit for unsymmetric load on the output partial voltages.

Fig.4(b) and/or Fig.4(c). For a given average current flow $I_{O,M,\mathrm{avg}}$ required by the load we have to adjust (as already mentioned) the average value

$$I_{M,\mathrm{avg}} = I_{O,M,\mathrm{avg}} \tag{15}$$

by a center point voltage control in a stationary mode. For the equivalent circuit according to Fig.4(a) there follows under consideration of the power balance between the mains and the DC sides

$$P_O = P_{O+} + P_{O-} = \frac{3}{2}\hat{U}_N \hat{I}_{N,(1)} \tag{16}$$

where P_{O+} denotes the load on U_{C+} and P_{O-} denotes the load on U_{C-} (the losses are neglected) and of the relation

$$I_{M,\mathrm{avg}}\frac{U_O}{2} = P_{O-} - P_{O+} \tag{17}$$

which corresponds to the node equation $I_{O,M,\mathrm{avg}} = I_{M,\mathrm{avg}} = I_{O-} - I_{O+}$,

$$I_{M,\mathrm{avg}} = \frac{3\hat{U}_N}{U_O}\hat{I}_{N,(1)}\, a_\mathrm{r} \,. \tag{18}$$

There,

$$a_\mathrm{r} = \frac{P_{O-} - P_{O+}}{P_O} = \frac{P_{O,\mathrm{a}}}{P_O} = \frac{\dfrac{P_{O,\mathrm{a}}}{P_{O,\mathrm{s}}}}{1 + \dfrac{P_{O,\mathrm{a}}}{P_{O,\mathrm{s}}}} \tag{19}$$

denotes the relative asymmetry of the loads P_{O+} and P_{O-} of the partial voltages U_{C+} and U_{C-}. $P_{O,\mathrm{s}}$ is the symmetric and $P_{O,\mathrm{a}}$ the asymmetric part of the overall output power

$$P_O = P_{O,\mathrm{s}} + P_{O,\mathrm{a}} \,. \tag{20}$$

For the equivalent circuit according to Fig.4(a) we have there

$$a_\mathrm{r} = \frac{R'_{L+} - R'_{L-}}{R'_{L+} + R'_{L-}} \,. \tag{21}$$

For the equivalent circuit according to Fig.4(b) we receive with

$$R'_{L+} = \frac{R_{L+-}}{2} \qquad R'_{L-} = \frac{R_{L+-}R_{L-}}{R_{L+-} + 2R_{L-}} \tag{22}$$

$$a_\mathrm{r} = \frac{R_{L+-}}{R_{L+-} + 4R_{L-}} \,. \tag{23}$$

For the equivalent circuit according to Fig.4(c) there follows with

$$R'_{L+} = \frac{R_{L+-}R_{L+}}{R_{L+-} + 2R_{L+}} \qquad R'_{L-} = \frac{R_{L+-}}{2} \tag{24}$$

$$a_\mathrm{r} = \frac{-R_{L+-}}{R_{L+-} + 4R_{L+}} \,. \tag{25}$$

Therefore, an entirely symmetric load on the partial voltages is characterized by $a_\mathrm{r} = 0$.

2.4 Analysis of the System Operating Behavior by Digital Simulation

In the following sections we will calculate (in a direct analytical way) the dependency of the global average value of the center point current i_M (cf. section 3) and of the harmonic rms value $\Delta I_{N,\mathrm{rms}}$ of the mains currents (cf. section 4) on the operating parameters and on the component characteristics. For the calculation of the stresses on the components in section 5 we use a digital simulation of the system behavior in those cases where an analytic calculation leads to relatively complex expressions (e.g., for the calculation of the current stress on the output capacitors). Furthermore, the digital simulation serves as a check for the results of the analytical calculations.

For the simulation parameters we select those rated quantities which are characteristic for an application of the system with the European low voltage mains (e.g., for application as input stage of an uninterruptible power supply (UPS), cf. section 3 in [9])

$$\begin{aligned} U_{N,\mathrm{rms}} &= 230\,\mathrm{V} \\ U_O &= 700\,\mathrm{V} \\ \hat{I}_N^* &= 18\,\mathrm{A} \\ f_P &= 16\,\mathrm{kHz} \\ L &= 1\,\mathrm{mH} \,. \end{aligned}$$

The relatively low value of the converter switching frequency $f_P = 16\,\mathrm{kHz}$ is set with respect to a short simulation time. A change of the modulation index (rated value $M = 0.93$) is obtained for constant output voltage U_O via changing the mains voltage amplitude $\hat{U}_N$. In order to point out the essential features we assume U_O to be impressed. This makes possible to avoid the design and simulation of the output voltage control loop. The guidance of the mains phase currents is realized by setting the space vector $\underline{u}_U^*$ (cf. Eq.(5)) which is present in the average over a pulse half period in such a way that the mains current space vector $\underline{i}_N$ is transferred from one point of the reference value circle $\underline{i}_N^*$ into a position which has a time difference of $\frac{1}{2}T_P$. One also can say that it is moved (seen as time average) along the reference value circle. This circle is defined by the fundamentals of the mains phase currents. By application of this predictive current control method according to the deadbeat principle we can avoid the calculation of an initial transient oscillation of the current control. Therefore, we can simulate the stationary operating behavior directly.

2.4.1 Normalization

In order to gain a far-reaching independency of the simulation results of the specific selected simulation parameters (or to gain results which are not limited to specific operating parameters and device characteristics) the calculated average and rms current values are related to the peak value $\hat{I}_N^*$ of the mains current reference value and/or the mains phase current fundamental $\hat{I}_{N,(1)} = \hat{I}_N^*$; for the normalized rms value of the power transistor current we have then, e.g.,

$$I_{T,\mathrm{rms,r}} = \frac{1}{\hat{I}_{N,(1)}} I_{T,\mathrm{rms}} \,. \tag{26}$$

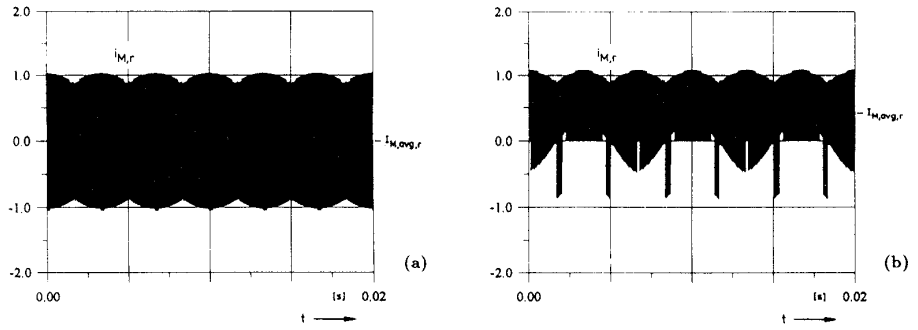

Fig.5: Simulation of the time behavior of the normalized center point current $i_{M,r}$ for $\rho_{--} = 0.5$ (cf. **(a)**) and $\rho_{--} = 0$ (cf. **(b)**). Simulation parameters according to section 2.4

The normalization basis of the rms value of the mains current harmonics $\Delta I_{N,\mathrm{rms}}$ is set to

$$\Delta I_r = \frac{U_O T_P}{8L} . \tag{27}$$

Then,

$$\Delta I_{N,\mathrm{rms},r} = \frac{1}{\Delta I_r} \Delta I_{N,\mathrm{rms}} \tag{28}$$

represents a characteristic value which is independent of $f_P = T_P^{-1}$ and of L in a first approximation.

3 Average Value of the Center Point Current and Maximum Allowable Load on the Output Voltage Center Point

As described in section 2.3 we have to form an average value $I_{M,\mathrm{avg}}$ of the center point current i_M for a load asymmetry a_r (cf. Eq.(15)). This is realized by proper influence of the time weighting and/or distribution ρ_{--} of the redundant switching states of the system. In connection with a practical application of the system we are interested in answering the question concerning the maximum allowable unsymmetry a_r (cf. Eq.(19)) of the load and/or the question regarding the maximum obtainable average value of the center point current.

As is immediately clear by Eq.(13) in connection with Tab.1, the positive maximum value of $I_{M,\mathrm{avg}}$ is formed for $\rho_{--} = 0$, the negative maximum value for $\rho_{--} = 1$. For illustrating the influence of the system behavior by the parameter ρ_{--} in **Fig.5** the time behavior of i_M is shown for $\rho_{--} = 0.5$ ($I_{M,\mathrm{avg}} \approx 0$) and $\rho_{--} = 0$.

In general we have for the global average value of the center point current

$$I_{M,\mathrm{avg}} = \frac{1}{\frac{2\pi}{3}} \int_0^{\frac{2\pi}{3}} i_{M,\mathrm{avg}}\{\varphi_U\}\, \mathrm{d}\varphi_U \tag{29}$$

(the considerations can be limited to $\frac{1}{3}$ of a mains period T_N (or 2π) due to symmetries of a three-phase system). There, for the local average value $i_{M,\mathrm{avg}}$ (related to a pulse half period) we have to use the determining equation which is valid in the respective integration interval. E.g., we have

$$i_{M,\mathrm{avg}} = \delta_{(010)} i_{N,S} + (1 - 2\rho_{--})(\delta_{(100)} + \delta_{(011)})\, i_{N,R} \tag{30}$$

for the integration interval lying in the partial triangle I pointed out in Fig.2.

Because the maximum values of the center point current are obtained for constant values of ρ_{--} ($\rho_{--} = 0$ or 1), we investigate in the following also the general dependency of $I_{M,\mathrm{avg}}$ on ρ_{--} and on the modulation index M for values $\rho_{--} \in [0,1]$ which are constant over φ_U. For a controls point of view we assume therefore a control of the center point current (and of the center point potential) with low dynamics.

Remark: By Eqs.(29) and (30) (and the further relations defining $i_{M,\mathrm{avg}}$ in the different integration intervals) an integration replaces the addition over single pulse half intervals which would actually have to be performed for the calculation of $I_{M,\mathrm{avg}}$. This makes possible an analytically closed calculation of the average value of the center point current. Because this approximation method is frequently applied for the analysis of the operating behavior of pulse converter systems (cf. e.g. [10]), we want to omit more detailed considerations here for the sake of brevity. The deviation of the analytical approximations in comparison to the results of a simulation is limited to a few percent for the ratio between pulse frequency and mains frequency $\frac{f_P}{f_N} = 500 \ldots 1000$ as being typical for a practical realization of the system. Therefore, the deviation can be neglected here.

If a purely sinusoidal shape of the mains current is assumed, we now can calculate directly the average value of i_M in dependency on the parameter ρ_{--} and on the modulation index M. After an involved calculation we receive

$$I_{M,\mathrm{avg},r} = \frac{3}{\pi}(1 - 2\rho_{--}) \tag{31}$$
$$\left[\, 1 + \frac{1}{2M}\left(\sqrt{3M^2 - 1} - \frac{1}{\sqrt{3}}\right) - \frac{\sqrt{3}M}{4}\left(1 + \frac{2\pi}{\sqrt{3}} - 2\sqrt{3}\,\arcsin\left(\frac{1}{\sqrt{3}M}\right)\right)\right] .$$

Eq.(31) represents a very good approximation of the exact dependency $I_{M,\mathrm{avg},r} = I_{M,\mathrm{avg},r}\{M, \rho_{--}\}$ which is shown in **Fig.6** and gained by digital simulation. For $\rho_{--} = 0.5$ in a first approximation the average value of the center point current is zero. According to Fig.6 $I_{M,\mathrm{avg},r}$ shows an approximately linear dependency on the control input ρ_{--} and on the modulation index M. The maxima of $I_{M,\mathrm{avg}}\{M\}$ resulting for $\rho_{--} = 1$ and $\rho_{--} = 0$ show equal absolute values. Therefore, basically a symmetric controllability $I_{M,\mathrm{avg}}\{\rho_{--}\} = -I_{M,\mathrm{avg}}\{1 - \rho_{--}\}$ is given. The decrease of the maximum obtainable average value with increasing M can be explained clearly by the fact that according to Eq.(7) with rising values of M the overall on-time of the redundant switching states is reduced. In general this also can be explained by the fact that forming of a high amplitude of the fundamentals of the phase voltages $u_{U,i}$ (high M) the current flow has to be provided especially via the positive or negative free-wheeling diodes $D_{F_i,+}$ or $D_{F_i,-}$. With this, the power transistors have only relatively short on-times. In the average, only a low contribution of the phase currents is fed into the center point. Therefore, it also becomes immediately clear that a direct connection between $I_{M,\mathrm{avg}}$ to the amplitude $\hat{I}_N$ of the mains current exists.

If one sets $\hat{U}_N \approx \hat{U}_{U,(1)}$ (i.e., if the voltage drop with mains frequency $\hat{U}_{L,(1)}$ across the series inductances L is neglected) one can calculate directly (by using the combination of Eqs.(18) and (31)) the maximum admissible relative asymmetry of the output power in dependency on the modulation index M and on the control input ρ_{--}, $a_{r,\max} = a_{r,\max}\{M, \rho_{--}\}$. (The voltage drop with mains frequency across the series inductances remains limited to a few percent of $\hat{U}_N$ for high pulse frequency and/or low values of the inductance L. Also, it has only little influence on the modulation index due to the geometric addition of the mains voltage and

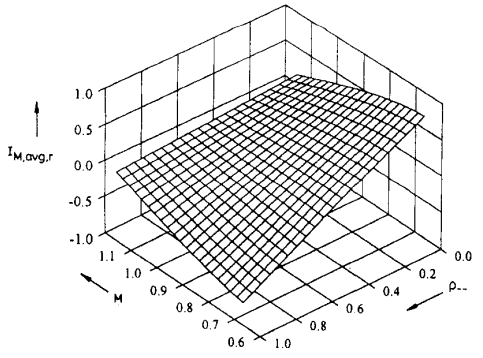

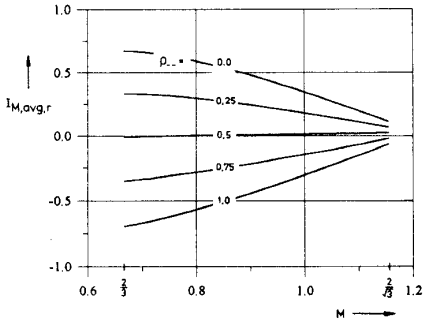

Fig.6: Dependency of the global normalized average value $I_{M,\mathrm{avg},r}$ of the center point current i_M on the modulation index M and the control input ρ_{--}.

the rectifier input voltage.) There follows

$$|a_r| \leq |a_{r,\max}| = |\frac{2}{\pi}(1-2\varrho_{--}) \quad (32)$$
$$[\frac{1}{M}+\frac{1}{2M^2}(\sqrt{3M^2-1}-\frac{1}{\sqrt{3}})-\frac{\sqrt{3}}{4}(1+\frac{2\pi}{\sqrt{3}}-2\sqrt{3}\arcsin(\frac{1}{\sqrt{3}M}))]|$$

(cf. **Fig.7**). As Fig.7 shows, a high asymmetry of the load is only possible for low modulation index and/or for output voltages U_O which are substantially higher than the peak value of the line-to-line mains voltage. Then there occurs a relatively high overall on-time of the redundant switching states. Therefore, a high average value $I_{M,\mathrm{avg}}$ can be generated by appropriate control input ρ_{--}. If now a maximum admissible asymmetry $|a_{r,\max}|$ is postulated during the course of dimensioning, for given mains voltage amplitude a minimum value of the output voltage is required thereby and/or the blocking voltage stress on the power semiconductors (ideally equal to half of the output voltage) is defined thereby.

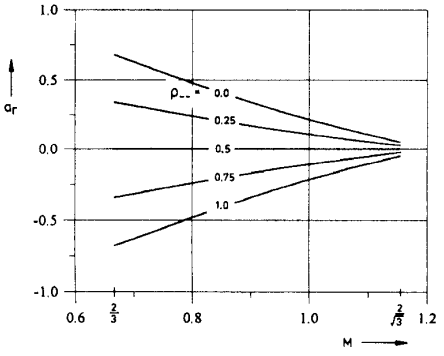

Fig.7: Absolute value of the admissible asymmetry $|a_r|$ of the load on the output partial voltages U_{C+} and U_{C-} (cf. Eqs.(19) and (32)) in dependency on the modulation index M and the control input ρ_{--}.

4 Influence of an Asymmetry of the Load on the RMS Value of the Mains Current Harmonics

The current consumption $\underline{i}_N$ of the rectifier system in general is determined by the difference of the mains voltage $\underline{u}_N$ and the rectifier input voltage $\underline{u}_U$

$$L\frac{\mathrm{d}\underline{i}_N}{\mathrm{d}t} = \underline{u}_N - \underline{u}_U \ . \quad (33)$$

In connection with Eq.(2) there follows therefore for the deviation

$$\Delta\underline{i}_N = \underline{i}_N - \underline{i}_N^* \quad (34)$$

of the actual mains current shape from the ideal sinusoidal form $\underline{i}_N^*$ the relation

$$L\frac{\mathrm{d}\Delta\underline{i}_N}{\mathrm{d}t} = \underline{u}_U^* - \underline{u}_{U,j} \ . \quad (35)$$

As Eq.(35) clearly shows, the harmonics with switching frequency of the mains current are caused be the difference between the space vector $\underline{u}_U^*$ (which has to be generated for a purely sinusoidal mains current shape) and the space vector $\underline{u}_{U,j}$ (which exists actually in the respective instant). By changing the time weight and/or the distribution ρ_{--} of the redundant switching states between begin and end of each pulse half period also the trajectory of the space vector $\Delta\underline{i}_N$ is influenced. Therefore, also the time shape of the ripple components of the mains phase currents is influenced. As will be shown in the following (and as also can be seen from **Fig.8**), a deviation from $\rho_{--} = 0.5$ in general leads to an increase of the ripple and/or the harmonic rms value $\Delta I_{N,\mathrm{rms}}$ of the mains phase currents. An asymmetric load on the output partial voltages therefore results basically in a deterioration of the mains behavior of the system.

In order to, e.g., make it possible (during the course of dimensioning) to quantify the influence of ρ_{--} on $\Delta I_{N,\mathrm{rms}}$ and/or on the normalized harmonic power loss (of one phase) as being characterized by $\Delta I_{N,\mathrm{rms}}^2$, in the following the dependency $\Delta I_{N,\mathrm{rms}}^2 = \Delta I_{N,\mathrm{rms}}^2\{M,\rho_{--}\}$ is analyzed in more detail. By considering the relation

$$\frac{3}{2}|\Delta\underline{i}_N|^2 = \Delta i_{N,R}^2 + \Delta i_{N,S}^2 + \Delta i_{N,T}^2 \quad (36)$$

the calculation of the sum of the squares of the local rms values of the ripple components of the mains phase currents

$$\Delta i_{N,RST,\mathrm{rms}}^2 = \frac{1}{\frac{1}{2}T_P}\int_{t_\mu=0}^{t_\mu=\frac{1}{2}T_P}(\Delta i_{N,R}^2 + \Delta i_{N,S}^2 + \Delta i_{N,T}^2)\mathrm{d}t_\mu \quad (37)$$

can be performed directly based on the trajectory which is defined by Eq.(35). For the switching state sequence (100)-(000)-(010)-(011) (cf. Fig.2) the corner points which are associated with the time values $t_{\mu,1}$, $t_{\mu,2}$ and $t_{\mu,3}$ of this triangular trajectory are defined by

$$\begin{aligned}\Delta\underline{i}_{N,t_{\mu 1}} &= \delta_{(100)}(\underline{u}_U^* - \underline{u}_{U,(100)})\\ \Delta\underline{i}_{N,t_{\mu 2}} &= \Delta\underline{i}_{N,t_{\mu 1}} + \delta_{(000)}(\underline{u}_U^* - \underline{u}_{U,(000)})\\ \Delta\underline{i}_{N,t_{\mu 3}} &= \Delta\underline{i}_{N,t_{\mu 2}} + \delta_{(010)}(\underline{u}_U^* - \underline{u}_{U,(010)}) \ .\end{aligned} \quad (38)$$

There,

$$\Delta\underline{i}_{N,t_\mu=0} = 0 \quad (39)$$

has to be assumed. If, in a first approximation, one assumes a motion of $\underline{i}_N^*$ in the direction of the tangent of the circular trajectory of $\underline{i}_N^*$, the origin is finally reached again for $t_\mu = \frac{1}{2}T_P$

$$\Delta\underline{i}_{N,t_\mu=\frac{1}{2}T_P} = 0 \ . \quad (40)$$

The basically interesting global (normalized) harmonic power loss of one phase follows via

$$\Delta I_{N,\mathrm{rms}}^2 = \frac{1}{2\pi}\int_0^{2\pi}\Delta i_{N,RST,\mathrm{rms}}^2\,\mathrm{d}\varphi_U \quad (41)$$

where the symmetries of a three-phase system are considered. As for the determination of the quantity $I_{M,\mathrm{avg}}$ related to the fundamental, also here the considerations can be limited to a third of the mains period. There follows

$$\begin{aligned}\Delta I_{N,\mathrm{rms,r}}^2 = \frac{3}{\pi}\Big\{&\sqrt{3}+\frac{16\pi}{9}-\frac{32}{9}\arcsin(\frac{1}{\sqrt{3}M})\\ &-2M(1+\frac{4}{\sqrt{3}}(1+\frac{22}{9}\sqrt{1-\frac{1}{3M^2}}))+M^2(6\sqrt{3}+\frac{28\pi}{3}-19\arcsin(\frac{1}{\sqrt{3}M}))\\ &+\frac{M^3}{2}(1-\frac{14}{3\sqrt{3}}(8+13\sqrt{1-\frac{1}{3M^2}}))+\frac{3M^4}{2}(\sqrt{3}+\pi)\\ &-6\varrho_{--}(1-\varrho_{--})[\frac{8}{9}(\sqrt{3}+\frac{7\pi}{6}-3\arcsin(\frac{1}{\sqrt{3}M}))\\ &-\frac{4M}{3}(-1+\frac{4}{\sqrt{3}}+\frac{11}{\sqrt{3}}\sqrt{1-\frac{1}{3M^2}})+M^2(\frac{13}{\sqrt{3}}+\frac{47\pi}{9}-14\arcsin(\frac{1}{\sqrt{3}M}))\\ &+\frac{M^3}{3}(17-2\sqrt{3}(8+11\sqrt{1-\frac{1}{3M^2}}))+\frac{M^4}{2}(3\sqrt{3}+\pi)]\Big\} \ .\end{aligned} \quad (42)$$

This relation (as shown graphically in **Fig.9**) is checked by a digital simulation. As Eq.(42) clearly shows, a harmonic-optimal control of the system is given for $\rho_{--} = 0.5$ (and/or for $I_{M,\mathrm{avg}} = 0$).

Remark: A further reduction of the harmonic losses can be obtained only by a change of the control parameter ρ_{--} over φ_N [11]. However, ρ_{--} has been assumed constant in this paper.

An asymmetric load on the system therefore basically results in an increase of

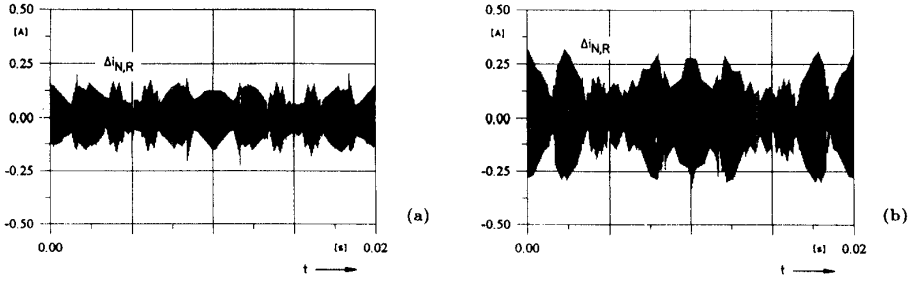

Fig.8: Simulation of the time behavior of the ripple $\Delta i_{N,R}$ of the mains current (in phase R) for $\rho_{--} = 0.5$ (cf. **(a)**) and $\rho_{--} = 1.0$ (cf. **(b)**); $U_{N,\mathrm{rms}} = 230\,\mathrm{V}$, $U_O = 700\,\mathrm{V}$ ($M \approx 0.93$); further simulation parameters as given in section 2.4.

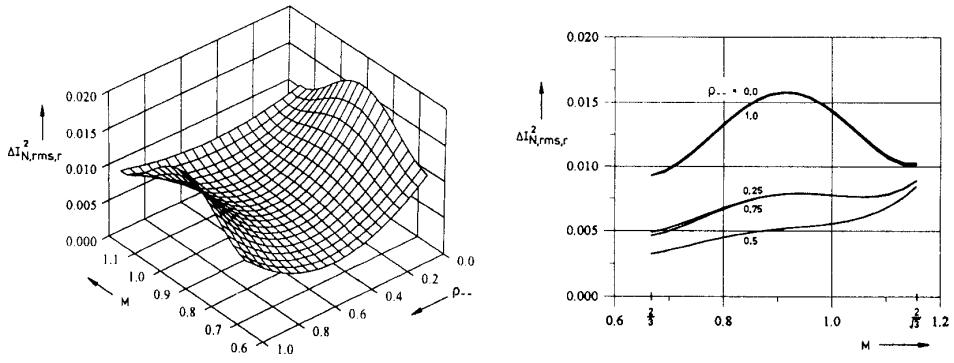

Fig.9: Analytically calculated dependency of the normalized (global) harmonic losses $\Delta I^2_{N,\mathrm{rms,r}}$ of a single phase in dependency on M and ρ_{--}.

the rms value of the mains current harmonics. For maximum admissible load asymmetry $|a_{r,\max}|$ ($\rho_{--} = 0$ or 1) the rms value of the harmonics of the mains current is increased for $M = \frac{2}{3} \ldots 1$ as compared to $a_r = 0$ and/or $\rho_{--} = 0.5$ by a factor of about $\sqrt{3}$. On the other hand, for high modulation indices (M close to $\frac{2}{\sqrt{3}}$) only a small increase of the harmonic rms value is given. This can be expained by the fact that (as already mentioned in connection with Eq.(31)) for increasing M the overall on-time of the redundant switching states is reduced. Therefore, *any* distribution ρ_{--} cannot take substantial influence on the shape of the trajectory Δi_N.

5 Stress on the Power Components for Asymmetric Loading of the Partial Output Voltages

As the considerations of section 3 show, by a change of ρ_{--} the main current flow is shifted from the positive to the negative (or from the negative to the positive) output voltage bus. Thereby, especially for small values of M and $\rho_{--} \approx 0$ or 1 a highly unsymmetric load on the power components of the positive and negative bridge halves results. For large modulation index M, ρ_{--} has relatively little influence on the stress on the devices due to the then relatively small overall on-time of the redundant switching states. In order to make possible a simple dimensioning of the rectifier system for asymmetric load, in the following the current stresses on the power semiconductors and on the output capacitors are compiled in normalized form for defined values of ρ_{--}.

5.1 Stresses on the Power Semiconductors

According to Fig.6(a), e.g., for $\rho_{--} > 0.5$ (and/or $a_r < 0$) a negative average $I_{M,\mathrm{avg}} < 0$ of the center point current results. Therefore, the asymmetric power flow takes place via the connection to the center point and the positive output voltage bus. As is immediately clear and as is shown in **Figs.10**(a) and 10(b) this leads to an increased stress on the free-wheeling diodes D_{F+} as compared to $\rho_{--} = 0.5$ (and/or $a_r = 0$); the stress on the free-wheeling diodes D_{F-} is reduced.

A corresponding consideration also gives a clear explanation for the increased stress for $\rho_{--} < 0.5$ on the center point diodes D_{M+} (which are located in the positive bridge half) as compared to diodes D_{M-} (cf. Figs.10(e) and 10(f)).

Regarding the mains current shape a change of ρ_{--} only influences the harmonic components of the mains phase currents, but not their sinusiodal shape (with mains frequency). The stress on the mains diodes D_{N+} and D_{N-} therefore also is not changed for asymmetric distribution of the output power as compared to $\rho_{--} = 0.5$ (and/or $a_r = 0$). In a first approximation we have independently of ρ_{--} (for purely sinusoidal main current shape $\hat{I}_N = \hat{I}_{N,(1)}$)

$$I_{D_N,\mathrm{avg,r}} = \frac{1}{\pi}$$
$$I_{D_N,\mathrm{rms,r}} = \frac{1}{2} \,. \qquad (43)$$

Also, the average value of the transistor current is not influenced by ρ_{--}. This is the case because for $\rho_{--} < 0.5$ the current in each phase flows within the positive half cycle of the related mains phase current in an increased amount via

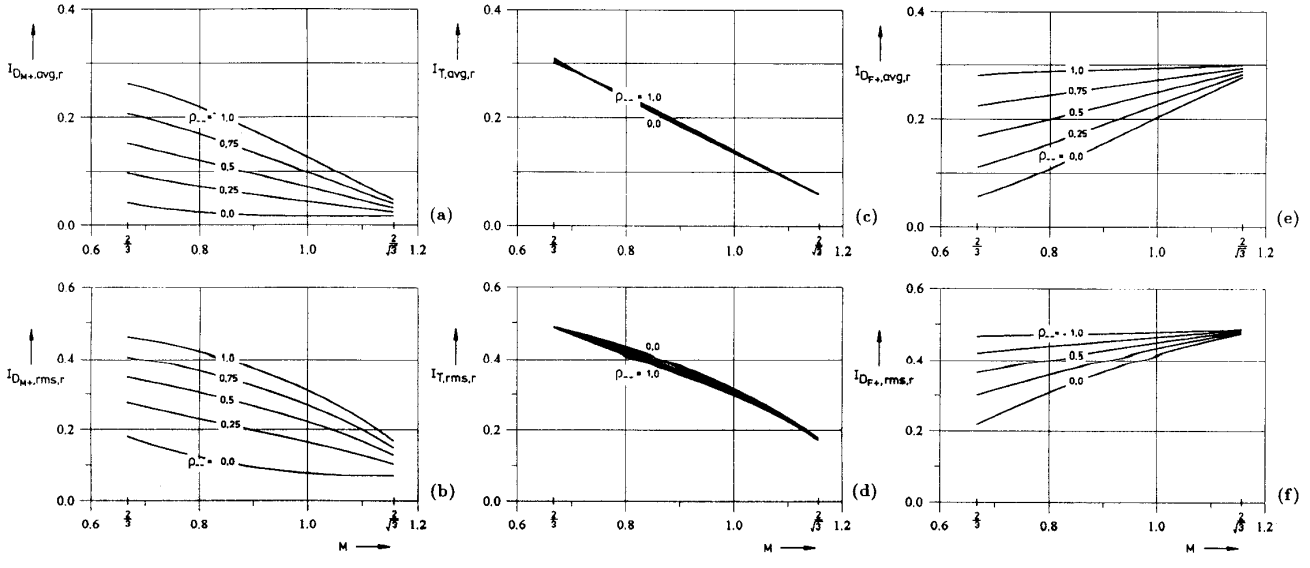

Fig.10: Dependency of the normalized average values and rms values of the currents in the power semiconductors on the modulation index M and on the distribution ρ_{--} of the overall on-time of the redundant switching states as determined by digital simulation. Free-wheeling diodes D_{F+} (cf. **(a)** and **(b)**), power transistors T (cf. **(c)** and **(d)**), center point diodes D_{M+} (cf. **(e)** and **(f)**). The characteristic values of the currents for the diodes D_{F-} and D_{M-} follow for a given value ρ_{--} by reading the characteristic values of the currents for D_{F+} and D_{M+} for a value $\rho'_{--} = (1 - \rho_{--})$.

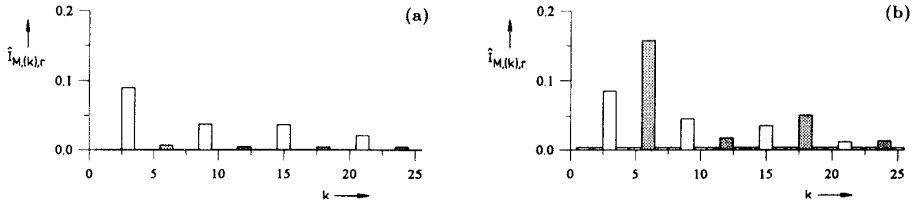

Fig.11: Amplitude spectrum of the center point current (normalized with respect to the amplitude of the mains current fundamental) as determined by digital simulation for $\rho_{--} = 0.5$ (cf. **(a)**) and $\rho_{--} = 0.0$ (cf. **(b)**).

D_{F+}, however within the negative half cycle it flows in an increased amout via the power transistor T. For the average of the transistor current we have in general

$$I_{T,\text{avg}} = 2I_{D_N,\text{avg}} - (I_{D_{F+},\text{avg}} + I_{D_{F-},\text{avg}}) \; . \tag{44}$$

As one can consider easily, the sum $I_{D_{F+}} + I_{D_{F-}}$ shows (independently of the load distribution) an always equal value. This value is determined (according to $P_O = 3\frac{U_O}{2}(I_{D_{F+},\text{avg}} + I_{D_{F-},\text{avg}})$) only by the overall output power P_O, the modulation index M and the amplitude of the mains phase currents. The transistor current average value therefore is independent of ρ_{--}; it is given by

$$I_{T,\text{avg},\text{r}} = (\frac{2}{\pi} - \frac{M}{2}) \tag{45}$$

(cf. Fig.10(c)).

According to Tab.1 during the presence of the redundant switching states currents of equal absolute value but of opposite sign are fed from one phase into the center point. (There, the current ripple is neglected.) As can be checked by Fig.10(d), a shift of the weighting ρ_{--} of the on-times of the redundant switching states therefore has no influence on the rms value of the transistor current (as determined by the square of the shape of the instantaneous current value). For the remaining dependency on the modulation index a more detailed analysis leads to

$$I^2_{T,\text{rms},\text{r}} = \frac{1}{2\pi}[\frac{7\pi}{6} + \frac{1}{3\sqrt{3}M^2} - \arcsin(\frac{1}{\sqrt{3}M}) - \frac{M}{2\sqrt{3}}(6\sqrt{3}-5) - \frac{2}{\sqrt{3}}(M + \frac{1}{6M})\sqrt{1-\frac{1}{3M^2}}] . \tag{46}$$

Remark: Concerning the basic dependency of the current stress on the power semiconductors on M we have to note that higher modulation indices are obtained in general by larger relative on-times of the free-wheeling diodes (and/or by shorter relative on-times of the power transistors). Therefore, with increasing M the current stress is transferred from the power transistors and center point diodes to the free-wheeling diodes.

5.2 Load on the Output Capacitors

The output capacitors C_+ and C_- of the system (which in general are realized as electrolytic capacitors) have to be dimensioned with respect to rms current stress and admissible (low-frequency) ripple of the center point potential. In order to not exceed a given maximum value of the amplitude $\hat{U}_{M,(k)}$ of a change of the capacitor voltage (as caused by the low-frequency harmonics $\hat{I}_{M,(k)}$ of the center point current) we have to select

$$C \geq \frac{1}{k\,\omega_N\,\hat{U}_{C,(k)}}\hat{I}_{C,(k)} \; . \tag{47}$$

($\hat{U}_{M,(k)}$ is set typically to $0.01U_O$.) There, k denotes the order of the current and voltage harmonics with respect to the mains frequency. For constant total output voltage U_O (controlled with high dynamics) a parallel connection of the output capacitors C_+ and C_- exists concerning the harmonics of the current i_M flowing into the center point M. Therefore, the center point current harmonics are divided into equal parts in both output capacitors (cf. Fig.15 in [12]). They shift the voltage center point, but they do not change to overall voltage U_O. Therefore, the harmonics of a capacitor current are to be calculated from the harmonics of i_M via

$$\hat{I}_{C,(k)} = \frac{1}{2}\hat{I}_{M,(k)} \; . \tag{48}$$

A typical spectrum of harmonics of i_M (where the DC term $I_{M,\text{avg}}$ is omitted) is shown in **Fig.11**. For symmetric control of the system ($\rho_{--} = 0.5$) the spectrum shows essential amplitudes of the harmonics only for ordinal numbers $k = 3, 9, 15, \ldots$ (odd multiples of 3, cf. Fig.11(a)); with increasing asymmetry of the control (i.e., $\rho_{--} \rightarrow 0$, cf. Fig.11(b), or $\rho_{--} \rightarrow 1$) the spectrum shows increasingly also harmonics for $k = 6, 12, 18, \ldots$ (even multiples of 3).

The dependency of the amplitudes of the low-frequency harmonics $k = 3, 6, 9$ (which are of special importance for the dimensioning) on the modulation index M and on the control parameter ρ_{--} is shown in **Fig.12**. Basically, ρ_{--} influences only the amplitudes of the even-order center point current harmonics. The amplitudes of the odd-order center point current harmonics remain unchanged in a first approximation. Besides the amplitudes of the harmonics of the center point and/or capacitor current also the rms value of the capacitor current influences the selection of the capacitance of the output (electrolytic) capacitors. The current stress resulting for C_+ in dependency on M and ρ_{--} is shown in **Fig.13**. For increasing unsymmetry of the load on the partial output voltages also the current stress on the output capacitors C_+ und C_- is changed in opposite directions. Only for symmetric load (and/or for $\rho_{--} = 0.5$) both capacitors have equal current stress

$$I^2_{C,\text{rms},\text{r}}|_{\rho_{--}=0.5} = \frac{10\sqrt{3}M}{8\pi} - \frac{9M^2}{16} \; . \tag{49}$$

6 Conclusions

As shown in this paper, by a proper distribution of the local overall on-time of the redundant switching states of a three-phase/switch/level PWM (VIENNA) rectifier system between begin and end of a pulse half period one can obtain a DC value $I_{M,\text{avg}}$ of the center point current which balances a load on the output voltage center point M. The sinusoidal shape of the mains current is not influenced thereby. The maximum value of the DC component is substantially determined by the modulation index M. For a value $M \approx 1$ (as being typical for application of the system with the European low-voltage mains) a control range of $I_{M,\text{avg}} \approx \pm 0.45 I_{N,\text{rms}}$ (cf. Fig.6) is given. (This means a very high asymmetric load capability of the rectifier system.) By the asymmetric control of the system the ripple of the mains current is increased as compared to symmetric control, however. The generation of the maximum (positive or negative) average value of the center point current is paid for by an increase of the rms value of the mains current ripple by a factor of $\approx \sqrt{3}$ for $M < 1.0$ (cf. Fig.9). Furthermore, an unsymmetric load on the output partial voltages always increases the load on the power semiconductors of one bridge half. The load on the other bridge half is reduced accordingly. An exception is given for the power transistors which have always the same stress, independently of the control mode (cf. Fig.10).

Finally we want to point out that one can easily influence the distribution of the on-time of the redundant switching states and/or the local average value $i_{M,\text{avg}}$ (which can be set directly for space vector modulation) also for application of a carrier modulation (or subharmonic) method (cf. Fig.4 in [13]). For this purpose one has to superimpose a zero-component onto the phase modulation functions (as described, e.g., in section IV in [14]). This quantity is equal for all phases and is not evident in the line-to-line rectifier input voltages; it only influences the distribution of the redundant switching states. The average value of the center

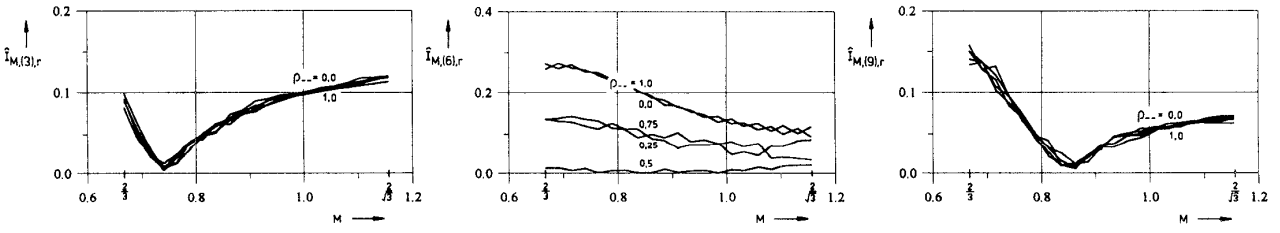

Fig.12: Dependeny of the amplitudes of the low-frequency harmonics (ordinal number (k), $k = 3, 6, 9$) of the center point current on the modulation index for different values of ρ_{--}, as determined by digital simulation.

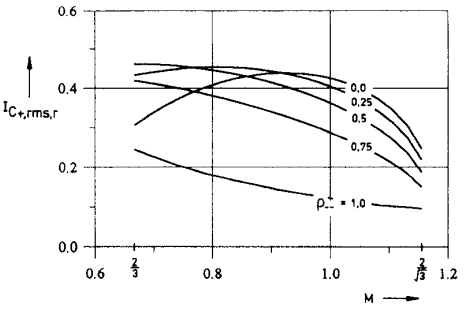

Fig.13: Dependency of the normalized value $I_{C+,\mathrm{rms},r}$ of the current in the output capacitor C_+ on the modulation index M and on ρ_{--}. The current load of C_- (associated with a value ρ_{--}) can be determined by reading the rms value $I_{C+,\mathrm{rms}}$ for $\rho'_{--} = (1 - \rho_{--})$.

point current $I_{M,\mathrm{avg}}$ (as being of interest in the case at hand) can be controlled in this case, e.g., by a DC component of the zero quantity.

ACKNOWLEDGEMENT

The authors are very much indebted to the *Hochschuljubiläumsstiftung der Stadt Wien* which generously supports the work of the Power Electronics Section at their university.

References

[1] **Kolar, J.W., and Zach, F.C.:** *A Novel Three-Phase Three-Switch Three-Level PWM Rectifier.* Proceedings of the 28th Power Conversion Conference, Nürnberg, Germany, June 28–30, pp. 125–138 (1994).

[2] **Kassakian, J.G.:** *High Frequency Switching and Distributed Conversion in Power Electronics.* Supplement to the Proceedings of the 6th Power Electronics and Motion Control Conference, Oct. 1–3, Budapest, Hungary (1990).

[3] **Kolar, J.W., and Zach, F.C.:** *A Novel Three-Phase Utility Interface Minimizing Line Current Harmonics of High-Power Telecommunications Rectifier Modules.* Record of the 16th IEEE International Telecommunications Energy Conference, Vancouver, Canada, Oct. 30– Nov. 3, pp. 367–374 (1994).

[4] **Zhao, Y., Li, Y., and Lipo, T.A.:** *Force Commutated Three-Level Boost Type Rectifier.* Conference Record of the 28th IEEE Industry Applications Society Annual Meeting, Toronto, Oct. 2–8, Pt. II, pp. 771–777 (1993).

[5] **Fukuda, S., and Sagawa, A.:** *Modelling and Control of a Neutral-Point-Clamped Voltage Source Converter.* Proceedings of the International Power Electronics Conference, Yokohama, Japan, April 3–7, Vol. 1, pp. 470–475 (1995).

[6] **Holtz, J.:** *Pulsewidth Modulation for Electronic Power Conversion.* Proceedings of the IEEE, Vol. 82, No. 8, pp. 1194–1214 (1994).

[7] **Kolar, J.W., Drofenik, U., and Zach, F.C.:** *Space Vector Based Analysis of the Variation and Control of the Neutral Point Potential of Hysteresis Current Controlled Three-Phase/Switch/Level PWM Rectifier Systems.* Proceedings of the International Conference on Power Electronics and Drive Systems, Singapore, Feb. 21–24, Vol. 1, pp. 22–33 (1995).

[8] **Rojas, R., Ohnishi, T., and Suzuki, T.:** *PWM Control Method for NPC Inverters with Very Small DC Link Capacitors.* Proceedings of the International Power Electronics Conference, Yokohama, Japan, April 3–7, Vol. 1, pp. 494–499 (1995).

[9] **Kolar, J.W., Drofenik, U., and Zach, F.C.:** *DC Link Voltage Balancing of Three-Phase/Switch/Level PWM (VIENNA) Rectifier by Modified Hysteresis Input Current Control.* Proceedings of the 30th International Power Conversion Conference, Nürnberg, Germany, June 20–22, pp. 443–465 (1995).

[10] **Kolar, J.W., Ertl, H., and Zach, F.C.:** *Calculation of the Passive and Active Component Stress of Three-Phase PWM Converter Systems with High Pulse Rate.* Proceedings of the 3rd European Conference on Power Electronics and Applications, Aachen, Germany, Oct. 9–12, Vol. III, pp. 1303-1311 (1989).

[11] **Kolar, J.W., Drofenik, U., and Zach, F.C.:** *AC- or DC-Side Optimum Stationary Operation of a High-Frequency Unidirectional Three-Phase Three-Switch Neutral Point Clamped PWM (VIENNA) Rectifier.* To be published at the 7th International Power Electronics & Motion Control Conference, Budapest, Hungary, Sept. 2–4 (1996).

[12] **Velaerts, B., Mathys, P., and Zendaoui, Z.F.:** *Study of 2 and 3-Level Precalculated Modulations.* Proceedings of the 4th European Conference on Power Electronics and Applications, Aachen, Germany, Vol. III, pp. 228–234 (1991).

[13] **Shimane, K., and Nakazawa, Y.:** *Harmonics Reduction for NPC Converter with a New PWM Scheme.* Proceedings of the International Power Electronics Conference, Yokohama, Japan, April 3–7, Vol. 1, pp. 482–487 (1995).

[14] **Ogasawara, S., and Akagi, H.:** *Analysis of Variation of Neutral Point Potential in Neutral-Point-Clamped Voltage Source PWM Inverters.* Proceedings of the 27th IEEE Industry Applications Society Annual Meeting, Toronto, Canada, Oct. 2–8, Pt. II, pp. 965–970 (1993).

[15] **Koczara, W.:** *Unity Power Factor Three-Phase Rectifier.* Proceedings of the 6th International (2nd European) Power Quality Conference, Munich, Germany, Oct. 14–15, pp. 79–88 (1992).